A Thermodynamic Database for $AlCl_3$-based Molten Salt Systems

C. Robelin, P. Chartrand and A.D. Pelton

Centre for Research in Computational Thermochemistry
École Polytechnique
Montréal (Québec), Canada, H3C 3A7

Chloroaluminate melts can be used as electrolytes for the production of aluminum and they are also involved in high energy density batteries ("Zebra" battery) : Na/β-Al_2O_3/$NaAlCl_4$, $FeCl_2$, Fe. Molten chlorides have many other industrial applications. For example, transition-metal chlorides are involved in the hot corrosion of metallic alloys. They are also used in the production of magnesium by electrolysis : the electrolyte is NaCl-KCl-$MgCl_2$-$CaCl_2$ and the transition-metal chlorides (mostly $MnCl_2$ and $FeCl_2$) are dissolved impurities.

A thermodynamic database has been developed for the LiCl-NaCl-KCl-$MgCl_2$-$CaCl_2$-$MnCl_2$-$FeCl_2$-$FeCl_3$-$CoCl_2$-$NiCl_2$-$AlCl_3$ system. All binary subsystems (except $AlCl_3$-$FeCl_3$) as well as all higher order (mostly ternary) subsystems for which experimental data were available have been considered. A complete critical evaluation of all available phase diagram and thermodynamic data (enthalpy of mixing, emf and vapor pressure measurements) has been performed for all condensed phases (liquid, solid solutions, stoichiometric compounds) and relevant gaseous species, and optimized model parameters have been found which best reproduce all the data simultaneously. In this way the data have been rendered self-consistent, discrepancies among the data have been identified, and extrapolations and interpolations have been performed. The models can be used with Gibbs free energy minimization software to calculate phase diagram sections, vapor pressures, and all thermodynamic properties at all compositions over extended ranges of temperature and pressure.

The thermodynamic optimizations of the LiCl-NaCl-KCl-$MgCl_2$-$CaCl_2$ [1] and NaCl-KCl-$MgCl_2$-$CaCl_2$-$MnCl_2$-$FeCl_2$-$CoCl_2$-$NiCl_2$ [2a,2b] systems have been published. The liquid solution was modeled using the Modified Quasichemical Model [3,4] which takes into account short-range ordering between second-nearest-neighbor cations. All relevant solid solutions were modeled using appropriate models. In particular, the $MgCl_2$-$MnCl_2$-$FeCl_2$-$CoCl_2$-$NiCl_2$ solid solution [2a,2b] was modeled using a cationic substitutional model with an ideal entropy and an excess Gibbs free energy expressed as a polynomial in the component mole fractions. The $(Li,Na,K)(Mg,Ca,Mn,Fe,Co,Ni)Cl_3$ and the $(Li,Na,K)_2(Mg,Mn,Fe,Co,Ni)Cl_4$ solid solutions were modeled using the Compound Energy Formalism [5].

Recently, the thermodynamic database for the LiCl-NaCl-KCl-$MgCl_2$-$CaCl_2$-$MnCl_2$-$FeCl_2$-$CoCl_2$-$NiCl_2$ system was extended with the addition of $AlCl_3$, and the thermodynamic optimization of the NaCl-KCl-$AlCl_3$ system was published [2c]. The binary systems *A*Cl-$AlCl_3$ (where *A* = Li, Na and K) show strong negative deviations from ideality at the equimolar composition (due to short-range ordering in the liquid phase), and the binary mixtures exhibit a region of liquid-liquid immiscibility at high $AlCl_3$ content. This is illustrated for the NaCl-$AlCl_3$ system in Figure 1, where the calculated phase diagram is compared with the available experimental data. The existence in *A*Cl-$AlCl_3$ melts of the $AlCl_4^-$ and $Al_2Cl_7^-$ species has been observed by Raman spectroscopy [6,7]. In order to introduce two different compositions of maximum short-range-ordering near the *A*$AlCl_4$ and *A*Al_2Cl_7 compositions, pure liquid aluminum chloride was modeled as a mixture of $AlCl_3$ and Al_2Cl_6 (with paired aluminum cations). Similarly, the $AlCl_3$-*M*Cl_2 systems (where *M* = Mg, Mn, Fe, Co and Ni) were modeled by introducing two different compositions of maximum short-range-ordering near the *M*$(AlCl_4)_2$ and *M*$(Al_2Cl_7)_2$ compositions. Satisfactory results were obtained in multi-component systems. This is illustrated in Figure 2, where the calculated section of the NaCl-KCl-$MgCl_2$-$AlCl_3$ phase diagram at constant weight ratio NaCl/KCl/$MgCl_2$ = 74.0/19.3/6.7 is compared with the available experimental data.

References

1. P. Chartrand and A.D. Pelton, *Metall. Mater. Trans.*, 2001, vol. 32A, pp. 1361-83.
2(a,b,c). C. Robelin, P. Chartrand and A.D. Pelton, *J. Chem. Thermodyn.* (in press).
3. A.D. Pelton, S.A. Degterov, G. Eriksson, C. Robelin and Y. Dessureault, *Metall. Mater. Trans.*, 2000, vol. 31B, pp. 651-9.
4. A.D. Pelton and P. Chartrand, *Metall. Mater. Trans.*, 2001, vol. 32A, pp. 1355-60.
5. B. Sundman and J. Ågren, *J. Phys. Chem. Solid*, 1981, vol. 42, pp. 297-301.
6. S.J. Cyvin, P. Klaeboe, E. Rytter and H.A. Øye, *J. Chem. Phys.*, 1970, vol. 52, pp. 2776-8.
7. H.A. Øye, E. Rytter, P. Klaeboe and S.J. Cyvin, *Acta Chem. Scand.*, 1971, vol. 25, pp. 559-76.

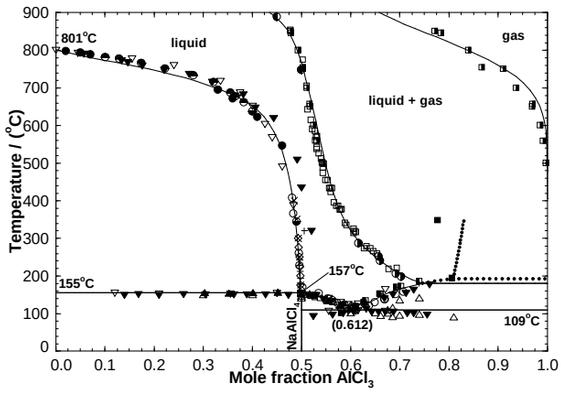

Figure 1 : Calculated NaCl-$AlCl_3$ phase diagram at 1 bar (dotted lines are liquid-liquid miscibility gap boundary and monotectic at *P* > 1 bar).

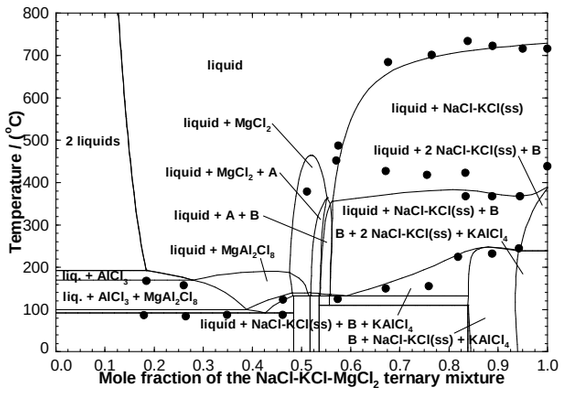

Figure 2 : Calculated section of the NaCl-KCl-$MgCl_2$-$AlCl_3$ phase diagram at constant weight ratio NaCl/KCl/$MgCl_2$ = 74.0/19.3/6.7 [A = $(Na,K)MgCl_3$(ss) and B = $(Na,K)_2MgCl_4$(ss)].